Finite Element Analysis of Six Transcortical Pin Parameters and Their Effect on Bone–Pin Interface Stresses in the Equine Third Metacarpal Bone

Timothy B. Lescun[1] Stephen B. Adams[1] Russell P. Main[2] Eric A. Nauman[3] Gert J. Breur[1]

[1] Department of Veterinary Clinical Sciences, College of Veterinary Medicine, Purdue University, West Lafayette, Indiana, United States
[2] Department of Basic Medical Sciences, College of Veterinary Medicine and Weldon School of Biomedical Engineering, College of Engineering, Purdue University, West Lafayette, Indiana, United States
[3] Weldon School of Biomedical Engineering, College of Engineering, Purdue University, West Lafayette, Indiana, United States

Address for correspondence Timothy B. Lescun, BVSc, PhD, Department of Veterinary Clinical Sciences, College of Veterinary Medicine, Purdue University, 625 Harrison Street, West Lafayette, IN 47909, United States (e-mail: tlescun@purdue.edu).

Vet Comp Orthop Traumatol 2020;33:121–129.

Abstract

Objective The objectives of this study were to validate a finite element model of the equine distal limb transfixation cast and to determine the effect of six transcortical pin parameters on bone–pin interface (BPI) stresses in the third metacarpal bone.

Study Design A transfixation cast finite element model was developed from a computed tomography scan of the third metacarpal bone and modelled pin elements. The model was validated by comparing strain measured around a 6.3-mm transfixation pin in the third metacarpal bone with the finite element model. The pin parameters of diameter, number, location, spacing, orientation and material were evaluated by comparing a variety of pin configurations within the model.

Results Pin diameter and number had the greatest impact on BPI stress. Increasing the diameter and number of pins resulted in lower BPI stresses. Diaphyseal pin location and stainless-steel pins had lower BPI stresses than metaphyseal location and titanium alloy pins, respectively. Offset pin orientation and pin spacing had minimal impact on BPI stresses during axial loading.

Conclusion The results provide evidence that diameter and number are the main pin parameters affecting BPI stress in an equine distal limb transfixation cast. Configurations of various pin size and number may be proposed to reduce BPI stresses and minimize the risk of pin related complications. Further refinement of these models will be required to optimize pin configurations to account for pin hole size and its impact on overall bone strength.

Keywords
- orthopaedics
- external skeletal fixation
- horse
- finite element
- pin
- stress

Introduction

Transfixation casting is a technique used to treat distal limb fractures in the horse.[1–3] Complications such as early pin loosening and secondary pin hole fracture impact clinical outcomes due to their common occurrence and potentially devastating consequences. Pin loosening is reported to occur in 68% of cases and secondary pin hole fractures occur in 14 to 20% of cases.[1,2] Transfixation casting is similar to external skeletal fixation and the reliance of both methods on the stability of the transcortical pin results in comparable limitations related to the bone–pin interface (BPI).[2,4,5] Pin loosening and pin hole

received
March 30, 2019
accepted after revision
October 3, 2019
published online
December 13, 2019

DOI https://doi.org/10.1055/s-0039-3399576.
ISSN 0932-0814.

fractures constitute a form of BPI failure, either insidiously for pin loosening or acutely for pin hole fracture. Local bone failure occurs when the yield stress threshold of the bone material is exceeded.[6] A reduction in pin related complications could be achieved by understanding and mitigating the factors contributing to BPI stress during transfixation casting.

The effect of altering parameters of external skeletal fixation on BPI stress has been examined using analytical, finite element (FE), ex vivo and in vivo methods in humans and small animals.[6–14] While some recommendations translate to transfixation casting, not all findings are expected to be applicable due to differences between the two techniques. Ex vivo studies of transfixation casting have evaluated parameters such as pin size, pin number, pin orientation, transcortical hole size, methods of cast attachment to pins and staged pin removal.[15–19] These studies address specific questions related to transfixation casting and help guide current clinical practice.[1,2,20] However, pin number and pin size were only evaluated in the radius, and transcortical hole size, pin orientation and staged pin removal have been evaluated in the third metacarpal bone. None of these studies examined the range of transcortical pin parameter values that could be modified nor did they evaluate the BPI. A systematic evaluation of specific transfixation pin parameters would provide clinicians with information regarding their effect on BPI stresses. We believe that similar to studies of external skeletal fixator systems,[8] determining which transcortical pin configurations minimize BPI stresses during transfixation casting could be used to guide clinical practices and help reduce the occurrence of pin related complications.

Finite element analysis has been utilized in orthopaedics prior to or in parallel with ex vivo and in vivo testing.[21–23] Utilizing FE analysis, the overall aim of our work was to evaluate a range of pin parameters and determine optimal configurations for the equine distal limb transfixation cast. The first objective of this particular study was to develop and validate an FE model representative of the equine distal limb transfixation cast. Our second objective was to utilize the model to determine the effect of six pin parameters on BPI stress and strain predictions in the equine third metacarpal bone. The results of this study will allow recommendations to be made regarding the effect of these pin parameters on anticipated BPI stresses during transfixation casting in the horse. The developed FE model will also provide a basis for future assessment of other parameters that determine the overall biomechanical performance of transfixation casts.

Materials and Methods

Study Design

An FE model of the equine third metacarpal bone was developed from computed tomography (CT) images of a cadaveric forelimb from a 10-year-old Quarter Horse gelding weighing 465 kg. The horse was owned by the university, had not been lame and was euthanatized for reasons unrelated to this study. The CT was performed from the carpus to the foot using a 64 slice helical scanner (Lightspeed VCT, General Electric, Milwaukee, Wisconsin, United States) at a slice thickness of 3.75 mm. Validation was performed by comparing FE analysis results with measured bone surface strain values obtained during ex vivo testing of the same third metacarpal bone with a single 6.3 mm transcortical pin.[21] Individual FE models were generated by combining the third metacarpal bone geometry with specific pin combinations to determine the effect of six different pin parameters on BPI stress and strain during axial loading.

Finite Element Model Construction

Models combining the third metacarpal bone and transcortical pins were constructed within an FE software programme (Abaqus, v.6.12; Dassault Systemes Simulia Corp, Rhode Island, United States). Slice geometry from the CT images was used to create the shape of the bone directly within the FE software programme using geometric part construction features and Boolean operations. The length of the third metacarpal bone model was 156 mm spanning from the proximal diaphysis to the physeal scar of the distal metaphysis. The cortical thickness varied from 15mm medially at the mid diaphysis to 7 mm laterally at the distal metaphysis. Pins were constructed to be 70 mm in length and were positioned within the bone model using Boolean operations. Non-linear surface to surface contact stiffness was applied at the BPI. This allowed separation of surfaces after contact, sliding between surfaces and prevented overclosure of surfaces under pressure. These conditions would be most representative of the BPI immediately after pin insertion. A 15 mm distance from the outer cortical bone margin to the fixed pin end was based on radiographic measurements from six previous clinical cases. To simulate standing and full weight shifting onto the limb, a 2500 N distributed axial compressive load was applied over the proximal surface of the third metacarpal bone. To simulate walking, a 7500 N distributed axial compressive load was applied to the proximal surface of the bone.[24] The material properties of the bone and pins used for the models were based on previous studies and reference data obtained from metal suppliers for pins (►**Table 1**).[25–28]

Free meshing algorithms were used and all models were meshed using solid quadratic tetrahedral elements (type C3D10I). Adaptive remeshing was performed to refine the mesh for each model based upon the output variable von

Table 1 Material properties of bone and metals used for FE modelling of transfixation pin combinations within the equine third metacarpal bone[25–28]

	Density (g/cm^3)	Elastic modulus (GPa)	Poisson's ratio
Cortical bone	2,000	17	0.3
Cancellous bone	500	0.5	0.3
Stainless steel	8,000	205	0.3
Titanium alloy	4,430	114	0.34

Abbreviation: FE, finite element.

Mises (VM) stress.[29] Remeshing was continued until the maximum change in VM stress from one mesh to the next fell below 2%, resulting in a stable mesh for analysis. The cast was not modelled and pin to cast attachment was restrained in all three axes as a boundary condition.[29] The distal end of the bone was unrestrained in the longitudinal axis while fully constrained in both transverse axes.

Model Validation

Validation was performed by comparing FE analysis to measured surface strains from ex vivo loading of the third metacarpal bone. A custom-made jig accommodated the bone and a single pin within the materials testing system (Qtest/50LP; MTS, Eden Prairie, Minnesota, United States) (►**Fig. 1**). A steel cap with a 5-mm deep, circular depression on the lower surface was placed over the proximal third metacarpal bone for loading. A solid steel cylinder 25 mm in length and 12 mm in diameter was positioned in a depression on the upper surface of the steel cap to transfer actuator load to the proximal bone surface.

A single smooth 6.3 mm diameter pin was inserted within the frontal plane 41 mm from the distal end of the bone segment following drilling of a transversely oriented 6.2 mm pin hole. Two rosette strain gauges (FRA-2-11; Texas Measurements, College Station, Texas, United States) were attached 5 mm from the hole margin at a proximal and a dorsal position for both lateral and medial holes. Longitudinally oriented single axis strain gauges (FLA-2-11) were placed in a palmar position 5 mm from the hole margins and on the dorsal midline 20 mm from the pin centre proximally and distally. Strain values in the longitudinal axis were obtained directly from the FE models and compared with those recorded during ex vivo testing (►**Fig. 2**). Axial compressive loads of 2500, 5000 and 7500N were applied sequentially at a loading rate of 6 mm/min. Load-deformation curves were generated to determine that each cycle of testing was within the linear elastic range of the bone. Maximum and minimum principal strain values were calculated using the rosette gauge data proximal to the medial and lateral pin holes[30] and compared directly to the corresponding values from the FE model.

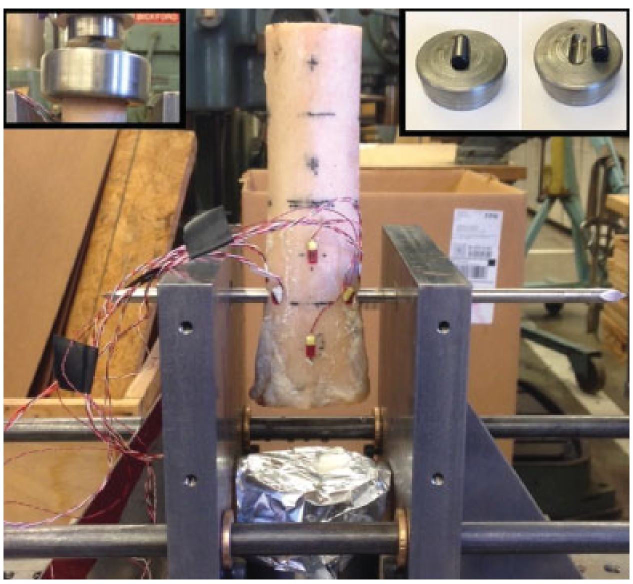

Fig. 1 Image of the custom jig used to perform axial compression testing. The bone and pin combination used for validation of the equine third metacarpal bone transfixation pin response under three separate loading conditions (2500 N, 5000 N and 7500 N) is shown. The lateral side of the bone is on the left side of the image. Strain gauges are attached to the dorsal bone surface and around both the medial and lateral pin holes. The insets show the loading cap design (right) and its positioning on the proximal bone surface (left) with the solid steel cylinder placed for even load transfer across the bone width from the material testing system load cell.

Pin Parameters

Six parameters of transfixation pins and their positioning in the third metacarpal bone were examined. The parameters were pin diameter, number, location, spacing, orientation and material. The specific variables evaluated for each parameter are presented in ►**Table 2**. All possible variable combinations (a total of 3,168 models) were not created. Specific comparisons were made between parameter variables while keeping other parameters of the models being compared constant. The combinations of pin diameter and pin number specifically evaluated are presented in ►**Table 3**. Pin location was evaluated by comparing single pins of various diameters positioned in either the diaphyseal or the metaphyseal region of the third metacarpal bone. Pin spacing and orientation were evaluated using a 6.3 mm pin diameter. Pin spacing was defined as the closest edge to edge distance between pins. An angle of 20 degrees from the frontal plane was used for positioning pins in an offset or divergent orientation (►**Fig. 3**). Stainless steel and titanium alloy pin materials were compared using single pins with diameters of 5, 6, 7, 8 and 9 mm positioned in the distal metaphyseal region of the third metacarpal bone.

Data Analysis

Output database files were generated for each FE model constructed. Specific data values recorded included the bone maximum and minimum principal stress and strain, maximum cortical bone VM stress and maximum pin VM stress. Direct comparisons between models were made to assess the impact of individual parameters. von Mises stress was used to report single parameter comparisons as it is a common predictor of yielding or material failure.[29] Stress and strain values were also examined for all parameter comparisons. Representative equations were developed to describe relationships between stress or strain and pin diameter or number. The Pearson product moment correlation coefficient was used to determine the best fitting equations describing the relationships observed.

Results

There were a total of 96 individual FE models constructed for the study. The number of models used to evaluate each of the pin parameters of interest are presented in ►**Tables 2** and **3**. The number of elements in the models ranged from approximately 25,000 up to 150,000; largely dependent upon the

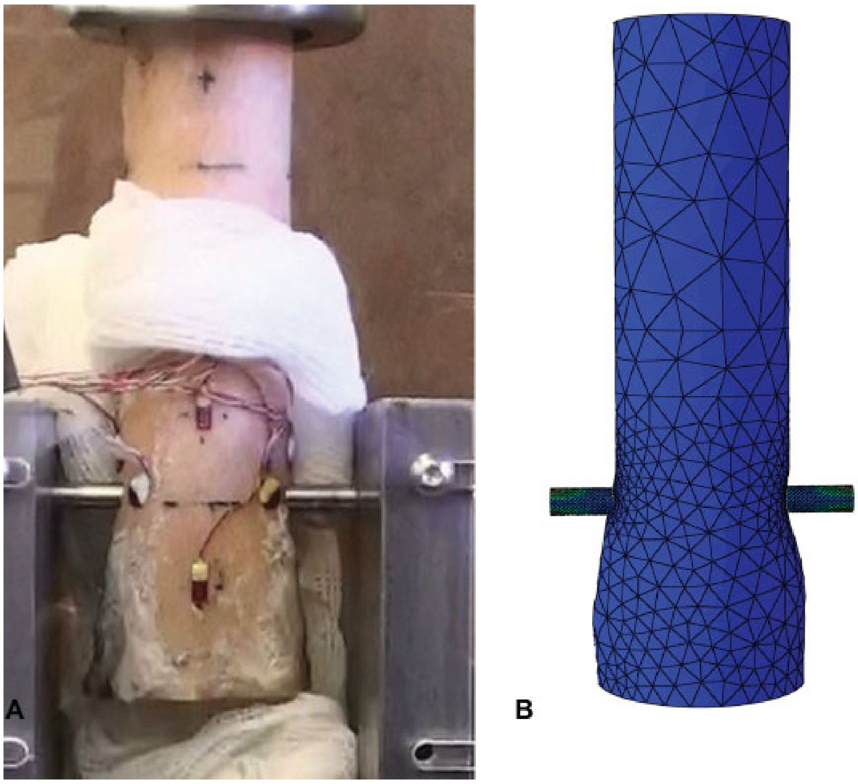

Fig. 2 Side by side comparison of ex vivo testing of a single 6.3-mm transcortical pin within the metaphyseal region of the third metacarpal bone of a horse for model validation and the comparable finite element model. (**A**) Equine third metacarpal bone with transcortical pin positioned in a custom testing jig and strain gages placed on the bone surface. (**B**) Finite element model geometry with a single 6.3-mm pin positioned in the metaphyseal region of the bone.

Table 2 Pin parameters for transfixation casting, the variables evaluated and the number of models generated to evaluate each parameter using FE analysis

Pin parameter	Variables	No. of models
Diameter (mm)	4, 5, 5.5, 6, 6.3, 7, 7.5, 8, 8.5, 9, 9.5	44
Number	1 to 6	44
Location	Diaphysis or metaphysis	17
Spacing (mm)	10, 20, 25, 30, 40, 50	12
Orientation	Inline or offset	12
Material	Stainless steel or titanium alloy	10

Abbreviation: FE, finite element.
Note: The models for the pin diameter and pin number are the same models. See ►**Table 3** for details.

Table 3 Table showing specific pin diameters (mm) and pin numbers for 44 FE models generated to examine the relationship between pin diameter and pin number

Diameter	4	5	5.5	6	6.3	7	7.5	8	8.5	9	9.5
Number 1	X	X		X	X	X	X	X	X	X	X
2	X	X		X	X	X	X	X		X	X
3	X	X		X	X	X	X	X		X	
4	X	X		X	X	X		X		X	
5	X	X		X		X		X			
6	X	X	X	X	X						

Abbreviation: FE, finite element.
Note: These models were all constructed with a 20-mm pin spacing, inline pin orientation and stainless-steel pin material.

number of pins included and the amount of remeshing required to achieve convergence of the models within the stated 2% limit for VM stress variation.

Model Validation

A similar linear response between the three load levels was observed in both the FE model and the bone–pin construct. Load, displacement and longitudinal strain values for both the ex vivo validation test procedure and the FE validation model are shown in ►**Table 4**. Comparison between the modelled and the measured strain values showed that measures were close to the x = y line representing complete agreement (►**Fig. 4**). The greatest deviations from the line were at the highest magnitude strain values, where the FE model tended to underestimate the calculated maximum principal strain and overestimate the calculated minimum principal strain. The linear regression line of best fit for the measured versus modelled values was $y = 0.962x - 88.7$ ($R^2 = 0.99$). Longitudinal strain values for the FE model varied from the corresponding measured values by a mean (±standard deviation) of 5.94 ± 5.88% across six measured sites (3 medial and 3 lateral). Maximum principal strain values, calculated from the rosette gauge measurements,

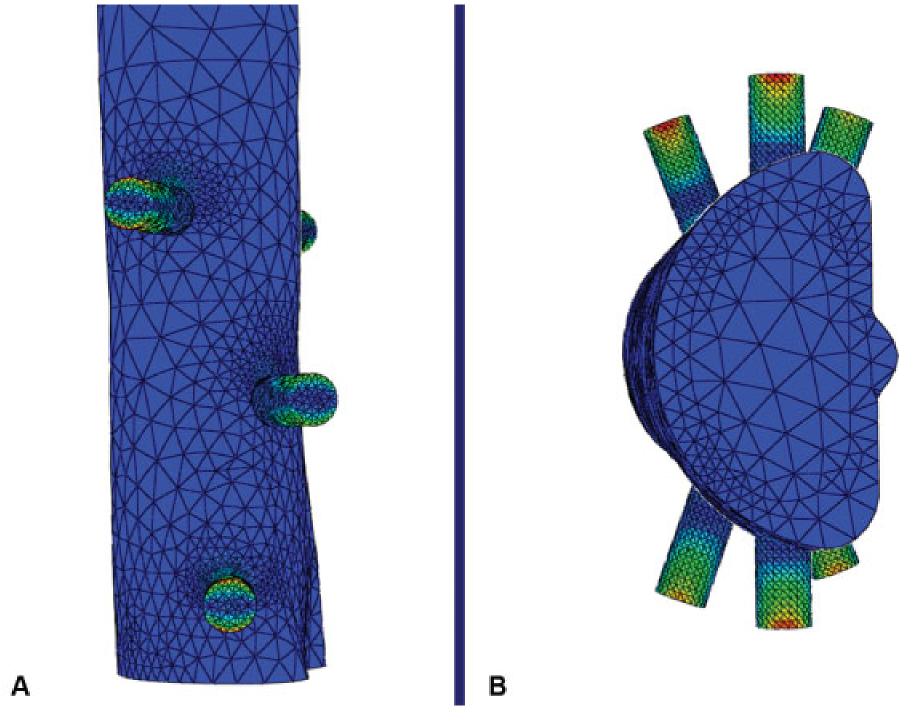

Fig. 3 (A) Image of the finite element model with three pins in an offset orientation as viewed from the medial aspect of the bone. (B) Same model as in A, viewed from the distal aspect of the bone to illustrate the angle of offset between pins.

Table 4 Load (N), displacement (mm) and longitudinal strain (microstrain) measured from an ex vivo cadaveric test and the comparable FE analysis predictions used for model validation at three different loads

Load			
Measured	2,502	5,013	7,502
Predicted	2,500	5,000	7,500
Displacement			
Measured	0.48	0.79	1.23
Predicted	0.43	0.80	1.18
Strain-medial hole			
Measured	−1,656	−2,788	−3,895
Predicted	−1,376	−2,751	−4,131
Strain-lateral hole			
Measured	−1,539	−3,239	−4,436
Predicted	−1,502	−3,008	−4,515

Abbreviation: FE, finite element.
Note: Negative values for strain represent compression.

varied from the corresponding FE model values by a mean of 10.03 ± 8.31%. Minimum principal strain values varied from the corresponding FE model by a mean of 7.33 ± 3.96%.

Pin Parameters

Pin diameter had a consistent effect on cortical bone VM stress, as well as principal stresses and strains. Smaller pin diameters resulted in higher stresses at the BPI. Maximum stress and strain values were invariably observed at the outer proximal margin of the pin hole and fell sharply both from the outer cortex toward the inner cortex and radially away from the edge of the pin hole (►**Fig. 5**). Pin number also had a consistent effect on maximum cortical bone VM stress. Increasing the number of pins resulted in a reduction in the maximum cortical bone VM stress values with a greater reduction for smaller pin diameters compared with larger pin diameters. The relationships between both pin diameter and pin number with maximum cortical bone VM stress are shown in ►**Fig. 6**.

Pin location was examined by comparing a range of pin sizes positioned in the diaphyseal region with corresponding pin sizes positioned in the distal metaphyseal region. Pin location in the distal metaphyseal region resulted in higher VM stress values than the diaphyseal region. This was more evident for smaller pin diameters (►**Fig. 7**). Small differences were observed between locations for maximum principal stress or maximum principal strain, while minimum principal stress and strain were lower in the metaphyseal region (i.e. higher compressive stress and strain) when compared with the diaphyseal region.

Pin spacing between two adjacent pins did not appreciably change stress patterns or their magnitude. Maximum cortical bone VM stress values varied by less than 4%, ranging from 247.7 to 257.2 MPa, over pin spacing distances ranging from 10 to 50 mm. Qualitative examination of the stress and strain patterns surrounding the pin holes did not show stress concentrations between or around pins for these spacing distances.

Comparisons were made between pins oriented in a divergent position 20 degrees from the frontal plane (offset) and pins oriented solely within the frontal plane (inline).

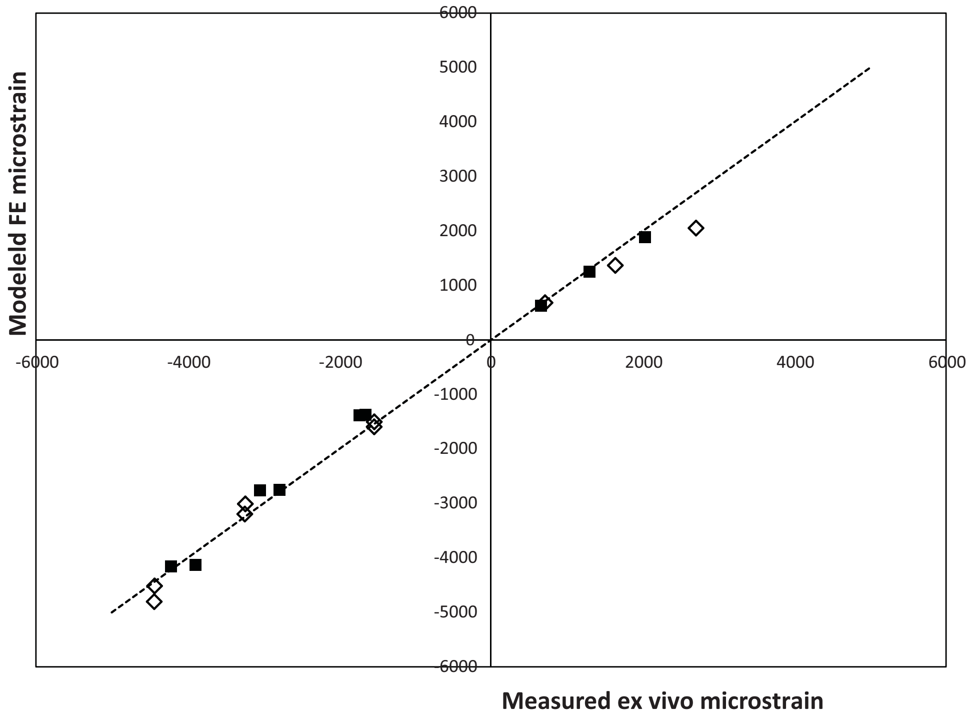

Fig. 4 Graph showing the comparison of measured ex vivo strain around medial (solid squares) and lateral (open diamonds) pin holes in third metacarpal bone compared with the modelled strain values from the corresponding finite element (FE) model. Data for longitudinal strain, maximum and minimum principal strains at loading levels of 2,500 N, 5,000 N and 7,500 N are shown as individual points on the graph. The dashed line is a plot of x = y to illustrate where exact matching between measured and modelled values lies.

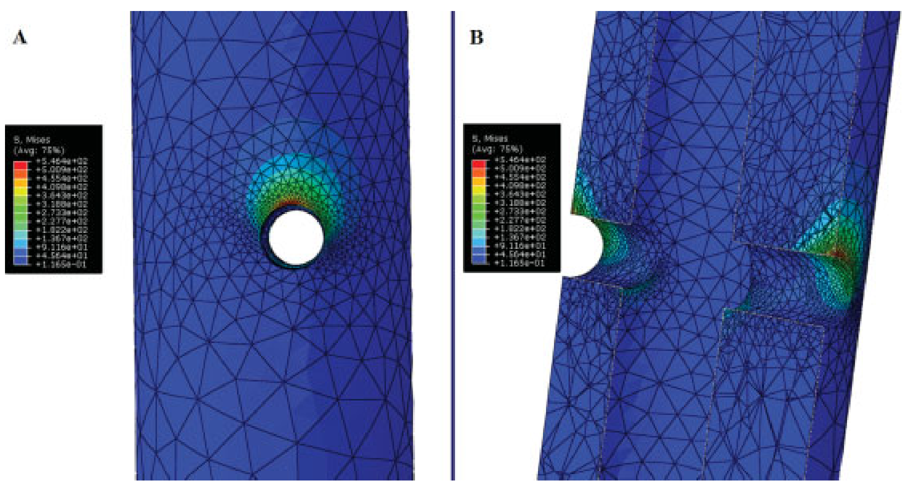

Fig. 5 Representative images showing the pattern of von Mises (VM) stress distribution surrounding a single smooth pin within the finite element model. Maximum VM stress is found at the proximal outer cortical margin of the pin hole. The legend shows the colour scale used to display VM stress. (**A**) View from the medial side of the bone model directly at the medial pin hole. (**B**) Sectioned view from the dorsal medial aspect of the bone showing the VM stress distribution within the medial and lateral cortices.

Offsetting the pin orientation in two and three pin models using 6.3 mm diameter pins resulted in similar values for maximum cortical bone VM stress, differing by less than 2% for both the two pin models (range from 243.4 to 247.7 MPa) and the three pin models (range from 163.3 to 166.3 MPa).

No consistent pattern of stress reduction or stress concentration was observed as a result of using an offset pin orientation.

Stainless steel and titanium alloy pins were compared using single pins positioned in the distal metaphyseal region. Maximum cortical bone VM stress with the stainless-steel pins was 26.9 to 37.0% lower than with the titanium alloy pins, while maximum pin VM stress for the titanium alloy pins was 4.7 to 9.1% lower than for the stainless-steel pins across the range of pin sizes examined.

Discussion

The purpose of this study was to develop and validate an FE model of the equine distal limb transfixation cast and use

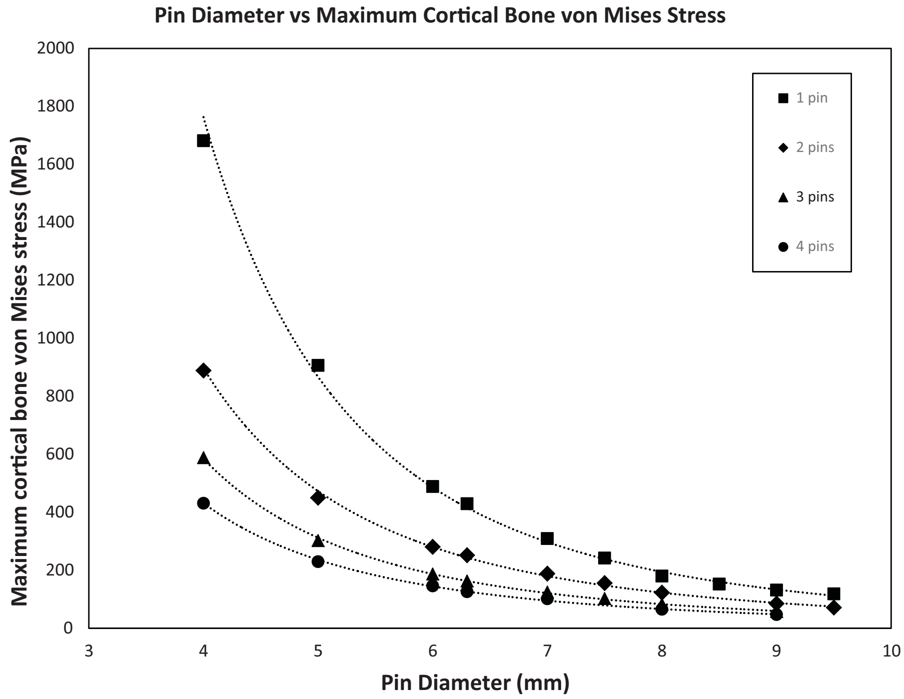

Fig. 6 Pin diameter versus maximum cortical bone VM stress for 34 individual finite element models evaluating pin diameter and pin number in the diaphyseal region of the third metacarpal bone. Solid squares = one pin models; solid diamonds = two pin models; solid triangles = three pin models; solid circles = four pin models.

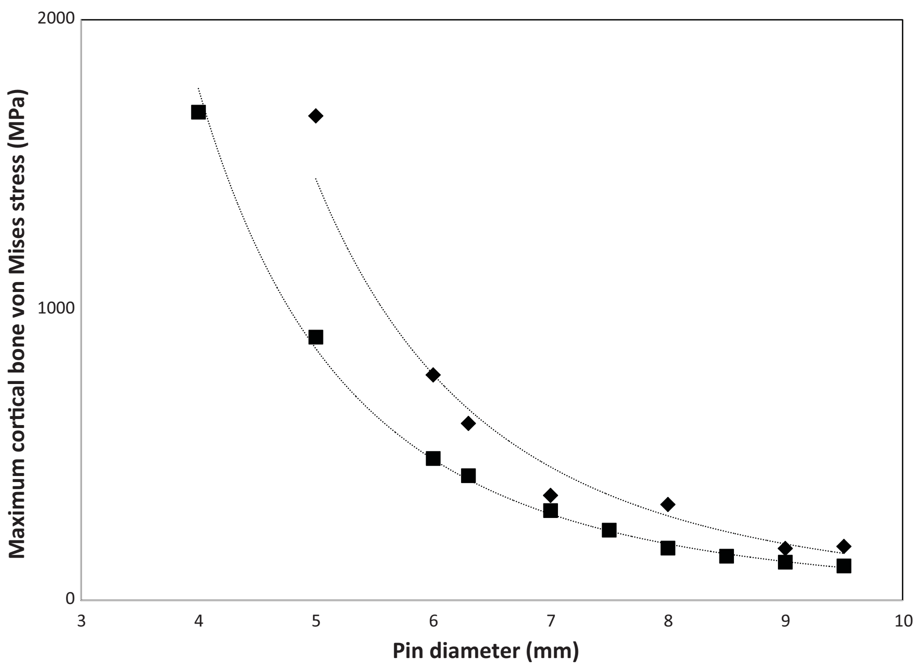

Fig. 7 Pin diameter versus maximum cortical bone von Mises stress for 17 individual finite element models with single pins positioned in the diaphyseal region (solid squares) or the metaphyseal region (solid diamonds) of the third metacarpal bone.

this model to systematically evaluate clinically relevant pin and pin positioning parameters to predict which combination(s) would result in reduced BPI stresses. The results show that the number of pins used in a transfixation cast, and their diameter, have the most profound effect on the BPI stresses and strains observed, consistent with previous studies examining external skeletal fixation parameters.[8,31] In contrast, both the spacing between pins and their orientation had minimal impact on BPI stress during axial loading. Pins located in the metaphyseal region of the bone resulted in higher compressive BPI stress than pins located in the diaphysis, which we attribute to the thinner cortical bone width present in the metaphyseal region.[8] Stainless-steel pins resulted in lower BPI stresses due to their higher stiffness; however, the titanium alloy pin stresses were lower than stainless-steel pins and as such may be less likely to break during cyclic loading, particularly as their yield stress is approximately four times higher than stainless-steel pins.[25,27] These results provide a basis from which pin configurations may be proposed that reduce BPI stress and strain in an equine distal limb transfixation cast.

Finite element analysis was used in this study because it can utilize the mechanical conditions of a system, calculate the predicted stress and strain environment of the system and provide data on specific models that can be further developed and refined, either with further FE analysis or by cadaveric or in vivo testing. This method of screening pin parameters avoided the use of a large number of animals or cadaver limbs. The conditions applied to the FE models in this study were designed to mimic the worst case-scenario of a horse walking with full weight on the cast limb with an axially unstable fracture.[24] Validation of the current model was performed by comparison to ex vivo testing on the same third metacarpal bone from which the model was based. The differences between the cadaveric and FE models were generally low, with only four specific comparisons having a difference greater than 10%, and the mean percentage differences across each of the strain measures analysed less than or equal to 10%. The simple shape of the equine third metacarpal bone allows good reproduction of its mechanical performance using FE models. Several investigators have used simple models of the equine third metacarpal bone and shown good agreement with ex vivo results.[24,32–34] These validation results support that the FE modelling approach had acceptable agreement with ex vivo testing.

The selection of parameters to evaluate in this study was based on current clinical practices. Pin diameters ranging in size from 4.7 to 9.5 mm have been reported clinically in adult horses.[1,2] Larger pin diameters are more resistant to bending and result in reduced BPI stress.[8] However, larger pins require larger holes in the bone cortex which has been shown to reduce the breaking strength of bone.[19,35,36] The area moment of inertia of the pin increases with the fourth power of the diameter. The relationship demonstrated between pin diameter and maximum VM stress for a single pin appears to be consistent with the influence that pin area moment of inertia is expected to have on bending stiffness of the pin and consequently BPI stress. It is evident from examining pin diameter against maximum cortical bone VM stress in the FE models with an increasing number of pins that the influence of pin diameter lessens as the number of pins increases. Further evaluation of the relationship between the area moment of inertia of the pin and the pin number is warranted as these parameters had the greatest influence on BPI stresses and strains.

Recommendations on pin location, made based on clinical observations, have been to place pins as far from the top of the cast as possible to avoid secondary pin hole fracture.[2,37] This approach results in pins located in the distal metaphysis of the third metacarpal bone. The results of the present study show that stress at the BPI would be expected to be lower in the diaphysis than the metaphysis. This suggests that previous clinical observations may be the result of factors other than high BPI stress contributing to an increased risk of secondary pin hole fracture for diaphyseal pin locations. The examination of pin orientation in this study failed to show a clear advantage of the method of offsetting pin positions from the frontal plane in the equine third metacarpal bone. However, our analysis used axial compression, while a previous study evaluating pin orientation in cadaveric bones used torsion and found that bone strength was greater with an offset orientation.[17] We elected to test in axial compression because that is the predominant load experienced by the third metacarpal bone in the horse.[24,33] The results of our study agree with clinical studies where neither pin loosening nor secondary pin hole fracture was found to be associated with an offset (divergent) pin orientation.[1,2]

There are several limitations of this study that merit discussion. Finite element analysis of mechanical behaviour requires the input of material properties, such as bone density and elastic modulus, and that several assumptions are made about the model. Bone is an anisotropic material and its density varies depending on the type of bone and its degree of porosity. A relationship between bone density and elastic modulus has been used to provide detailed material information on an elemental level to increase the accuracy of an FE model.[38] However, this method of material assignment increases the computational complexity of the model substantially. The assumption that the pin ends are completely fixed is unlikely to reflect the true situation within a cast. Further evaluation of the effect of this assumption on the results of these models is warranted. Another limitation in this study was the fact that the BPI contact conditions were simplified by not accounting for BPI friction. Friction would be expected to have an effect on lateral to medial sliding of the pin even though the major loading direction is normal to the pin surface. In our models, sliding was unable to occur as the pin ends were fixed in position.

The main advantage of using the simplified modelling approach was the ability to make multiple comparisons across different pin parameters. Coupled with validation of the model, these findings provide a basis from which to investigate additional aspects of the equine transfixation cast which are likely to influence BPI stress using further ex vivo and in vivo testing. Ultimately, identifying ideal pin parameter combinations, such as pin size and number, which minimize BPI stresses and strains, should reduce the likelihood of both acute and chronic BPI failure and improve the safety of the equine distal limb transfixation cast during clinical use.

Authors' Contributions

Timothy Lescun contributed to conception of study, study design, acquisition of data and data analysis and interpretation. Stephen Adams and Eric Nauman contributed to conception of study and study design. Russell Main contributed to acquisition of data and data analysis and interpretation. Gert Breur contributed to conception of study, study design and data analysis and interpretation. All authors drafted, revised and approved the submitted manuscript.

Funding
This study was supported by the State of Indiana and the Purdue University School of Veterinary Medicine Research account funded by the Total Wagers Tax.

Conflict of Interest
None declared.

Acknowledgments
The authors acknowledge Anirban Mahato and Kari Jensen for technical assistance with mechanical testing.

References

1 Joyce J, Baxter GM, Sarrafian TL, Stashak TS, Trotter G, Frisbie D. Use of transfixation pin casts to treat adult horses with comminuted phalangeal fractures: 20 cases (1993-2003). J Am Vet Med Assoc 2006;229(05):725–730
2 Lescun TB, McClure SR, Ward MP, et al. Evaluation of transfixation casting for treatment of third metacarpal, third metatarsal, and phalangeal fractures in horses: 37 cases (1994-2004). J Am Vet Med Assoc 2007;230(09):1340–1349
3 Kraus BM, Richardson DW, Nunamaker DM, Ross MW. Management of comminuted fractures of the proximal phalanx in horses: 64 cases (1983-2001). J Am Vet Med Assoc 2004;224(02):254–263
4 McClure S, Honnas CM, Watkins JP. Managing equine fractures with external skeletal fixation. Compend Contin Educ Pract Vet 1995;17:1054–1063
5 Clary E, Roe S. Enhancing external skeletal fixation pin performance - consideration of the pin-bone interface. Vet Comp Orthop Traumatol 1995;8:6–13
6 Aro HT, Markel MD, Chao EY. Cortical bone reactions at the interface of external fixation half-pins under different loading conditions. J Trauma 1993;35(05):776–785
7 Pettine KA, Chao EY, Kelly PJ. Analysis of the external fixator pin-bone interface. Clin Orthop Relat Res 1993;(293):18–27
8 Huiskes R, Chao EY, Crippen TE. Parametric analyses of pin-bone stresses in external fracture fixation devices. J Orthop Res 1985;3(03):341–349
9 Bouvy BM, Markel MD, Chelikani S, Egger EL, Piermattei DL, Vanderby R Jr. Ex vivo biomechanics of Kirschner-Ehmer external skeletal fixation applied to canine tibiae. Vet Surg 1993;22(03):194–207
10 Wu JJ, Shyr HS, Chao EY, Kelly PJ. Comparison of osteotomy healing under external fixation devices with different stiffness characteristics. J Bone Joint Surg Am 1984;66(08):1258–1264
11 Chao EY, Aro HT, Lewallen DG, Kelly PJ. The effect of rigidity on fracture healing in external fixation. Clin Orthop Relat Res 1989;(241):24–35
12 Aro HT, Kelly PJ, Lewallen DG, Chao EY. The effects of physiologic dynamic compression on bone healing under external fixation. Clin Orthop Relat Res 1990;(256):260–273
13 Aro HT, Chao EY. Biomechanics and biology of fracture repair under external fixation. Hand Clin 1993;9(04):531–542
14 Liu RW, Kim YH, Lee DC, Inoue N, Koo TK, Chao EY. Computational simulation of axial dynamization on long bone fractures. Clin Biomech (Bristol, Avon) 2005;20(01):83–90
15 Hopper SA, Schneider RK, Ratzlaff MH, White KK, Johnson CH. Effect of pin hole size and number on in vitro bone strength in the equine radius loaded in torsion. Am J Vet Res 1998;59(02):201–204
16 McClure SR, Watkins JP, Hogan HA. In vitro evaluation of four methods of attaching transfixation pins into a fiberglass cast for use in horses. Am J Vet Res 1996;57(07):1098–1101
17 McClure SR, Watkins JP, Ashman RB. In vitro comparison of the effect of parallel and divergent transfixation pins on breaking strength of equine third metacarpal bones. Am J Vet Res 1994;55(09):1327–1330
18 Williams JM, Elce YA, Litsky AS. Comparison of 2 equine transfixation pin casts and the effects of pin removal. Vet Surg 2014;43(04):430–436
19 Seltzer KL, Stover SM, Taylor KT, Willits NH. The effect of hole diameter on the torsional mechanical properties of the equine third metacarpal bone. Vet Surg 1996;25(05):371–375
20 Rossignol F, Vitte A, Boening J. Use of a modified transfixation pin cast for treatment of comminuted phalangeal fractures in horses. Vet Surg 2014;43(01):66–72
21 Burkhart TA, Andrews DM, Dunning CE. Finite element modeling mesh quality, energy balance and validation methods: a review with recommendations associated with the modeling of bone tissue. J Biomech 2013;46(09):1477–1488
22 Huiskes R, Hollister SJ. From structure to process, from organ to cell: recent developments of FE-analysis in orthopaedic biomechanics. J Biomech Eng 1993;115(4B):520–527
23 Taylor M, Prendergast PJ. Four decades of finite element analysis of orthopaedic devices: where are we now and what are the opportunities? J Biomech 2015;48(05):767–778
24 Les CM, Stover SM, Taylor KT, Keyak JH, Willits NH. Ex vivo simulation of in vivo strain distributions in the equine metacarpus. Equine Vet J 1998;30(03):260–266
25 Chen Q, Thouas GA. Metallic implant biomaterials. Mater Sci Eng Rep 2015;87:1–57
26 Stevenson M, Barkey M, Bradt R. Fatigue failures of austenitic stainless steel orthopedic fixation devices. Pract Fail Anal 2002;2:57–64
27 Anonymous. Product Data Sheet - 316/316L Stainless Steel. 2007. Available at: www.aksteel.com
28 McClure SR, Glickman LT, Glickman NW, Weaver CM. Evaluation of dual energy x-ray absorptiometry for in situ measurement of bone mineral density of equine metacarpi. Am J Vet Res 2001;62(05):752–756
29 Brianza S, Brighenti V, Lansdowne JL, Schwieger K, Bouré L. Finite element analysis of a novel pin-sleeve system for external fixation of distal limb fractures in horses. Vet J 2011;190(02):260–267
30 Biewener AA. In vivo measurement of bone strain and tendon force. In: Biewener AA, ed. Biomechanics–Structures and Systems: A Practical Approach. New York: IRL Press at Oxford University Press; 1992:123–147
31 Huiskes R, Chao EY. Guidelines for external fixation frame rigidity and stresses. J Orthop Res 1986;4(01):68–75
32 Les CM, Keyak JH, Stover SM, Taylor KT. Development and validation of a series of three-dimensional finite element models of the equine metacarpus. J Biomech 1997;30(07):737–742
33 Merritt JS, Burvill CR, Pandy MG, Davies HM. Determination of mechanical loading components of the equine metacarpus from measurements of strain during walking. Equine Vet J Suppl 2006;(36):440–444
34 Merritt JS, Pandy MG, Brown NAT, et al. Mechanical loading of the distal end of the third metacarpal bone in horses during walking and trotting. Am J Vet Res 2010;71(05):508–514
35 Kuo RF, Chao EY, Rim K, Park JB. The effect of defect size on the stress concentration and fracture characteristics for a tubular torsional model with a transverse hole. J Biomech 1991;24(02):147–155
36 Hipp JA, Edgerton BC, An KN, Hayes WC. Structural consequences of transcortical holes in long bones loaded in torsion. J Biomech 1990;23(12):1261–1268
37 Németh F, Back W. The use of the walking cast to repair fractures in horses and ponies. Equine Vet J 1991;23(01):32–36
38 Schileo E, Taddei F, Cristofolini L, Viceconti M. Subject-specific finite element models implementing a maximum principal strain criterion are able to estimate failure risk and fracture location on human femurs tested in vitro. J Biomech 2008;41(02):356–367